Phase Transition in Swollen Gels. 21. Effect of Acrylamide Quaternary Salts with Various Alkyl Lengths on the Collapse, Mechanical, and SAXS Behavior of Poly(acrylamide) Networks

M. Ilavský,*,†,‡ Z. Sedláková,‡ K. Bouchal,‡ and J. Pleštil‡

Faculty of Mathematics and Physics, Charles University, 180 00 Prague 8, Czech Republic, and Institute of Macromolecular Chemistry, Academy of Sciences of the Czech Republic, 162 06 Prague 6, Czech Republic

Received February 24, 1995; Revised Manuscript Received June 20, 1995[⊗]

ABSTRACT: A series of ionic networks were prepared by copolymerization of acrylamide, methylenebis(acrylamide), and *N*-[2-(alkyldimethylammonio)ethyl]acrylamide with C1, C4, C6, C8, C12, and C16 straight-chain alkyls (mole fraction of the last comonomer $x_I = 0-0.15$). Small-angle X-ray scattering, swelling, and mechanical behavior of the networks were investigated in water–ethanol mixtures. For the gels with C1–C8 alkyls collapse was found; both the volume jump and the critical ethanol concentration at which the transition takes place, e_c, increase with increasing content of the ionic component, x_I. Increasing the alkyl length stabilizes the expanded state of the gel and increases the e_c values, probably due to preferential sorption of ethanol by hydrophobic regions. Different swelling behavior was found for gels with C12 and C16 alkyls, where mostly a decrease in swelling in water at low ethanol concentrations was observed with increasing x_I. This is caused by a distinct amphiphilic character of salts with the two longest alkyls; in networks with the C16 alkyl formation of micelles was proved by SAXS. Mechanical behavior of the networks is predominantly determined by the degree of swelling; a jumpwise change in the gel volume is accompanied by a similar change in the equilibrium modulus.

Introduction

A number of swollen polymer networks carrying a low amount of charges on the chain (1–15 mol %), when subjected to a change of the external parameters (composition of the solvent, temperature, electric field, and the like), undergo a first-order phase transition (collapse), at which the change in volume may range from 10 to 1000 times.[1–5] This transition is given by a change of the chain conformation: SANS experiments showed that in the expanded state the chains have a coil shape, while in the collapsed state they are in compact globular structures.[6] The extent of the collapse is affected by molecular parameters of the networks[3] (cross-linking density, dilution at network formation, charge concentration). It has been proved, both experimentally[1–5] and theoretically,[7] that electrostatic interactions of charges on the chain have a great influence on the existence and extent of the transition. Besides these, also other fundamental interactions, such as van der Waals forces, hydrogen bonding, and hydrophobic interactions, determine the phase behavior and conformation of the chains at the collapse. The jump in volume is accompanied by a jump in other physical characteristics of the gel, such as shear modulus, refractive index, stress-optical coefficient, and the like.[3] Due to these changes the gels showing the collapse are being considered for use in various devices,[8–12] sensors, artificial muscles, mechanochemical actuators, etc.

Hydrophobic interactions, which are due to an ordered structure of water molecules in the vicinity of hydrophobic parts of the polymer chain,[13] also affect the extent of the collapse. These interactions play an important role in biopolymers and in the collapse caused by the change of temperature in poly(*N*,*N*-diethylacrylamide)[14] and poly(*N*-isopropylacrylamide)[4,15] hydrogels. The increasing length of alkyl in the side group of the chains is the way to control hydrophobic interactions in the system.

In this study we investigate the effect of concentration of acrylamide quarternary salts with various lengths of alkyl on the collapse and mechanical behavior of poly(acrylamide) (PAAm) networks prepared by the copolymerization of AAm with the salts and a cross-linker. The advantage of such systems consists in that the degree of ionization is virtually pH-independent and the length of alkyl in salts affects the extent of hydrophobic interactions. Due to a distinct amphiphilic character of salts (especially with long alkyls), formation of micelles can be expected. Therefore, also the SAXS experiments on selected systems were carried out.

Experimental Section

Sample Preparation. Five acrylamide quarternary ammonium salts **I** with various lengths of the alkyl substituent

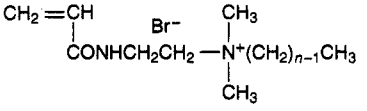

I; n = 4, 6, 8,12, and 16

were synthesized. The salts were prepared by quaternization of [2-(acrylamido)ethyl]dimethylamine with alkyl bromides (C4, C6, C8, C12, and C16 straight-chain alkyls) in acetonitrile. The quaternization reaction proceeded 72 h at 25 °C; the salts C4 and C6 precipitated during the reaction; the other salts were precipitated by dry ether. Characterization of quarternary salts **I** (C*n*, mp, analysis % Br(exp)/% Br(theor), yield (%)): C4, 170 °C, 28.6/28.7, 95; C6, 74 °C, 25.8/26, 92; C8, 93 °C, 23.7/23.9, 75; C12, 81 °C, 20.5/20.4, 70; C16, 80 °C, 18/17.9, 62.

Five series of ionic networks, copolymers of acrylamide (AAm), cross-linker *N*,*N*′-methylenebis(acrylamide) (MBAAm), and salt **I** (n = 4, 6, 8, 12, and 16) with mole fraction of **I**, x_I, ranging from 0 to 0.15, were prepared. The samples were polymerized from 100 mL of an aqueous solution which contained 0.135 g of MBAAm (0.88 mmol), 0.02 g of ammonium

† Charles University.
‡ Academy of Sciences of the Czech Republic.
⊗ Abstract published in *Advance ACS Abstracts,* August 15, 1995.

0024-9297/95/2228-6835$09.00/0

Table 1. Network Characteristics and Collapse Parameters

x_I	G_1 (g cm^{-2})	$10^5\nu_d$ (mol cm^{-3})	$\Delta \log X$	$\Delta \log G$	e_c (vol %)	Q_w	ϕ
			Series C4				
0	32.8	2.6				34	
0.005	32.0	2.54				35	0.2
0.01	34.4	2.73				43.5	0.17
0.02	28.0	2.22	0.76	0.25	50	71	0.13
0.05	39.4	3.12	1.20	0.46	65	418	0.22
0.10	34.8	2.76	1.65	0.51	75	500	0.17
0.15	35.0	3.56	1.80	0.69	80	556	0.18
			Series C6				
0.005	33.0	2.61				36	0.12
0.01	37.1	2.93				39	0.13
0.02	41.0	3.25				76	0.17
0.05	37.1	2.93	1.12	0.32	71	378	0.18
0.10	29.1	2.30	1.58	0.57	79	518	0.15
0.15	36.2	2.85	1.80	0.62	83	500	0.13
			Series C8				
0.005	84.0	2.69				36	0.10
0.01	32.5	2.58				37	0.05
0.02	38.1	3.02				60	0.10
0.05	38.7	3.07	1.04	0.40	72	267	0.10
0.10	42.7	3.38	1.44	0.53	80	385	0.18
0.15	36.4	2.88	1.62	0.60	85	425	0.13
			Series C12				
0.005	26	2.06				50	0.2
0.01	28	2.22				41	0.03
0.02	36	2.85				31	
0.05	28	2.22				32	
0.10	25	1.98				60	0.02
0.15	29	2.30				62	0.01
			Series C16				
0.005	29	2.31				75	0.45
0.01	32	2.54				42	0.03
0.02	35	2.77				40	0.01
0.05	70	5.58				14	
0.10	78	6.22				13	
0.15	73	5.78				31	
			Series C1[a]				
0.012	34	3.66	0.9	0.35	45	56	0.25
0.024	38	4.10	1.25	0.45	50	159	0.35
0.050	32	3.44	1.60	0.60	55	417	0.23
0.090	33	3.56	1.90	0.60	60	522	0.18
0.164	31	3.34	1.95	0.60	65	632	0.18

[a] Data taken from ref 16.

peroxodisulfate, 150 μL of *N,N'*-tetramethylethylenediamine (TEMED), and 7 mmol of a mixture of AAm and **I** to obtain the mole fraction of **I** in the copolymers x_I = 0.005, 0.01, 0.02, 0.05, 0.10, and 0.15 (Table 1). All ingredients, with the exception of TEMED, were dissolved in water, and the solutions were flushed with nitrogen for 10 min, after which TEMED was added. The polymerization proceeded at room temperature for 24 h in ampules of diameter D^* = 10 mm. After the polymerization, the samples were extracted in redistilled water for 7 days.

Swelling and Mechanical Measurements. After extraction the samples were immersed in water–ethanol mixtures. Swelling proceeded for ~28 days, after which the inverse swelling ratio X relative to the state at network formation was determined from[17]

$$X = (D^*/D)^3 = V^*/V \quad (1)$$

where D^* and D respectively are the sample diameters after the preparation and swelling and V^* and V respectively are the corresponding sample volumes. The diameters were measured with an Abbé comparator (Zeiss Jena, accuracy ±0.02 mm). From the X values it is easy to calculate the volume fraction of the polymer in the swollen state, v_2 ($v_2 = v^0X$, where v^0 is the fraction of the polymer at network formation, v^0 = 0.04), and the swelling degree relative to the dry state, Q ($Q = 1/v_2 = 25/X$).

The deformational measurements were carried out on cylindrical specimens in a uniaxial compression in an earlier described apparatus.[17] The specimen, ~10–20 mm high, was compressed to a ratio Λ (Λ = l/l_0, where l and l_0 respectively are the deformed and the initial height of the specimen) and the force f was measured after 30 s of relaxation. Usually 10 Λ_i and f_i values were determined in the range 0.8 < Λ_i < 1. From these values the equilibrium shear modulus G was determined from the relation

$$G = f/S_0(\Lambda^2 - \Lambda^{-1}) \quad (2)$$

in which S_0 is the initial cross section of the specimen. The measurements were carried out with both samples just after preparation (modulus G_1) and samples swollen to equilibrium in water–ethanol mixtures (modulus G). Using the modulus G_1, the concentration of elastically active network chains related to the dry state ν_d was calculated from

$$\nu_d = G_1/RTv^0 \quad (3)$$

where R is the gas constant and T is the temperature (T = 298 K). In Table 1 the basic network characteristics and parameters of collapse found earlier[16] for the copolymer containing **I**, n = 1, are shown (denoted as series C1). In series C1 swelling and mechanical measurements were carried out in water–acetone mixtures.[16]

Small-Angle X-ray Scattering Measurements. SAXS experiments were done by using a Kratky camera (Anton Paar KG, Graz, Austria) with a linear position-sensitive detector[18] (Joint Institute for Nuclear Research, Dubna, Russia). Scattering curves were converted to the absolute scale by means of Lupolen standards, using the formula[19]

$$\frac{d\tilde{\Sigma}}{d\Omega}(q) = \frac{a}{\tilde{I}_L K_L T_s d}\tilde{I}(q) \quad (4)$$

where $\tilde{I}(q)$ is the measured scattering intensity, a is the sample–detector distance, T_s is the sample transmission, d is the sample thickness, K_L is a calibration constant, $\tilde{I}_L$ is the intensity of radiation scattered by the standard at $q = (2\pi/150\ \text{Å})$, $q = (4\pi/\lambda)\sin\theta$ is the magnitude of the scattering vector, λ is the wavelength of radiation, and 2θ is the scattering angle. The differential scattering cross section $d\tilde{\Sigma}(q)/d\Omega$ in reciprocal centimeters can then be obtained by means of the desmearing programs ITP or ITR.[20]

Development of the network structure during the polymerization reaction was studied in time-resolved SAXS experiments. The minimum time for one frame was 100 s. This time was chosen to be comparable to that elasped between the addition of the TEMED into the polymerization mixture and the start of data acqusition.

Results and Discussion

Swelling and Mechanical Characteristics. A continuous or jumpwise decrease in the macroscopic volume of the gel (increase in the inverse swelling ratio X) with increasing volume fraction of ethanol, e, in the water–ethanol mixtures is observed for all the series, C4–C16 (Figures 1–5). While for series C4, C6, and C8 the first-order phase transition (jumpwise change in X) can be found, for series C12 and C16 only a continuous increase in X with increasing e is detected for all the **I** concentrations, x_I. Table 1 and Figures 1–3 show that the critical salt concentration x_I^c at which the networks undergo phase transition slightly increases with increasing length of the alkyl (x_I^c = 0.012, 0.02, 0.05, and 0.05 for series C1, C4, C6, and C8, respectively). As expected, a jumpwise change in the volume of the gel is reflected also in a jumpwise change in the shear modulus G (Figures 1–3). For network series C12 and C18 a continuous dependence of X on e is accompanied by a continuous dependence of the shear

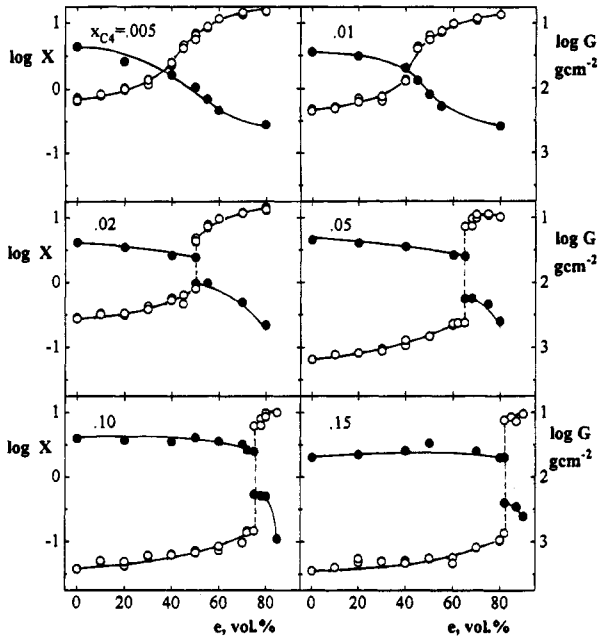

Figure 1. Dependence of the swelling ratio, X, and modulus, G (g cm^{-2}), on the concentration of ethanol, e (vol %), in network series C4: (○) X; (●) G. The numbers correspond to the mole fraction of **I**, x_I.

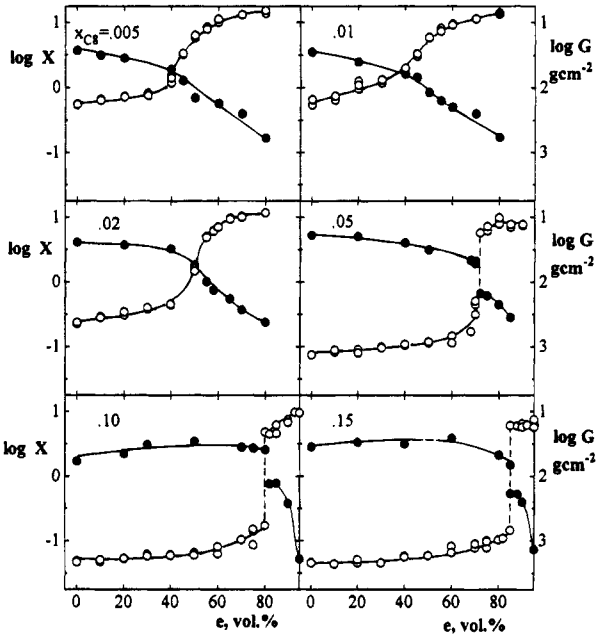

Figure 3. Dependence of the swelling ratio, X, and modulus, G (g cm^{-2}), on the concentration of ethanol, e (vol %), in network series C8: (○) X; (●) G. The numbers correspond to the mole fraction of **I**, x_I.

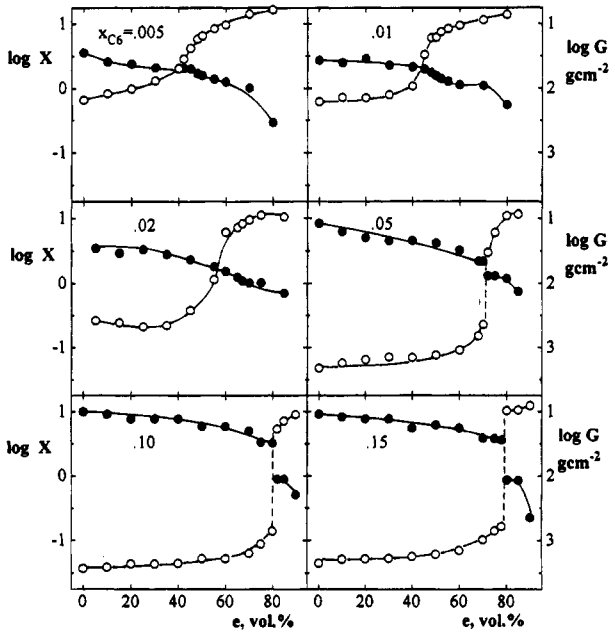

Figure 2. Dependence of the swelling ratio, X, and modulus, G (g cm^{-2}), on the concentration of ethanol, e (vol %), in network series C6: (○) X; (●) G. The numbers correspond to the mole fraction of **I**, x_I.

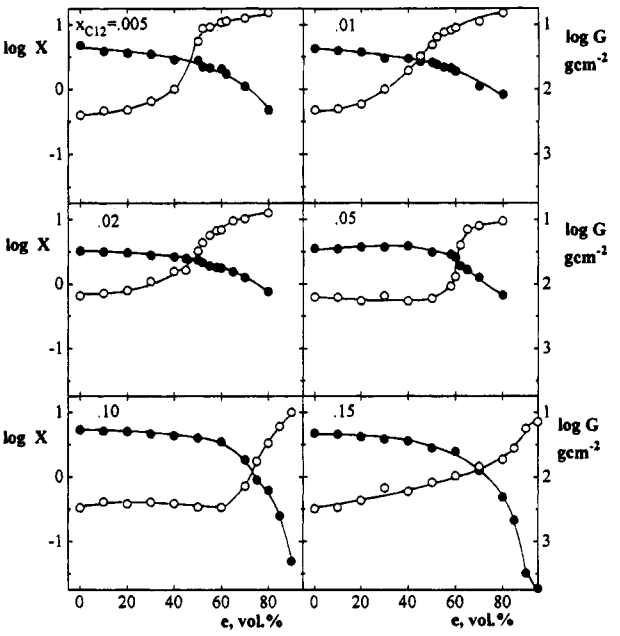

Figure 4. Dependence of the swelling ratio, X, and modulus, G (g cm^{-2}), on the concentration of ethanol, e (vol %), in network series C12: (○) X; (●) G. The numbers correspond to the mole fraction of **I**, x_I.

modulus G on e for all salt concentrations (Figures 4 and 5).

The dependences of the modulus G on the swelling ratio X are shown in Figure 6 for gel series C4, C8, and C16. Qualitatively similar results were obtained for network series C6 and C12. As the constant amount of cross-linker was used in all series the modulus data lie roughly on the same log G vs log X dependence regardless of **I** concentrations for individual series. Despite large scatter, in the middle range of swelling the log G values increase with log X with the predicted rubber elasticity[21] slope $s = 0.33$ for all the series. Departures from the straight line in the range of high swelling (log $X < -1$) are probably due to the finite extensibility of the chains, while those in the range of low swelling (log $X > 0.75$) are due to the influence of the main transition region (vitrification) at high ethanol concentrations.[17]

The value of the slope $s = 0.33$ differs from the slope $s = 0.65$ found earlier for ionic PAAm networks prepared by the copolymerization of AAm with sodium methacrylate[17] (MNa) and ionic poly(*N*,*N*-diethylacrylamide) (PDEAAm) networks prepared[14] from DEAAm and MNa. On the other hand, for variously aged PAAm networks the value of $s = 0.45$ was found.[22] A high value of $s \simeq 0.7$ was also found[23] for positively charged PAAm networks if the positive charge of the quaternary ammonium group was attached to the main chain through the ester group. From the results presented

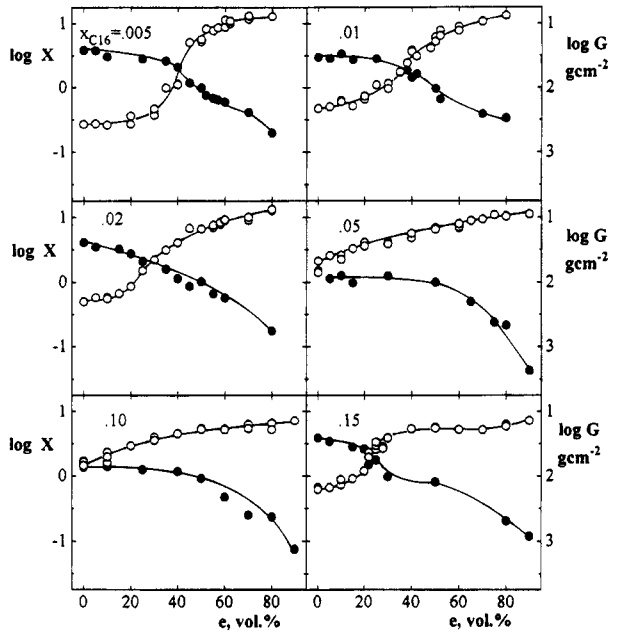

Figure 5. Dependence of the swelling ratio, X, and modulus, G (g cm^{-2}), on the concentration of ethanol, e (vol %), in network series C16: (○) X; (●) G. The numbers correspond to the mole fraction of **I**, x_I.

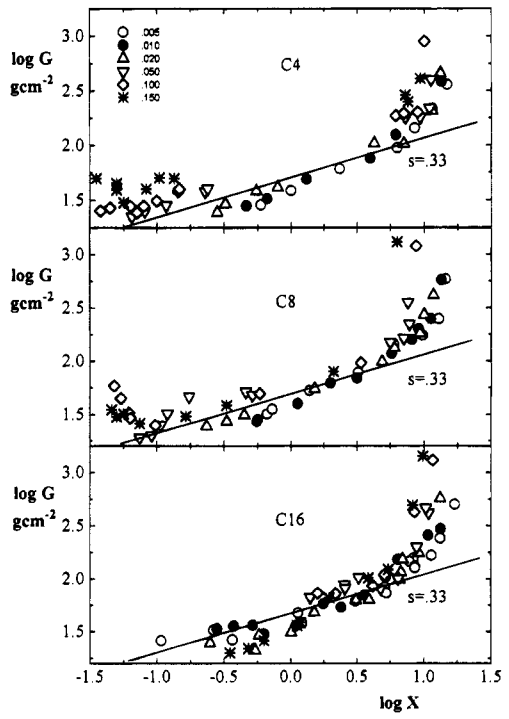

Figure 6. Dependence of the modulus G on the swelling ratio, X, for variously ionized gel series C4, C8, and C16.

in Figure 6 it follows that the attachment of the positive charge to the main chain through the amide group decreases the s value (see also the results[16] obtained for series C1).

The jump in the volume of the gel may be characterized by the extent of the collapse $\Delta \log X$ (=$\log X'' - \log X'$, where X' is the swelling ratio of the expanded state of the gel and X'' is the ratio after the collapse; Figure 1). According to Figure 7, the jumpwise change in the moduli $\Delta \log G$ in series C1, C4, C6, and C8 adequately correlates with the jump in the swelling ratio (and, hence, in volume) of the gel $\Delta \log X$ ($\Delta \log G = 0.33\Delta$ log X) with earlier found slope $s = 0.33$. Thus, from

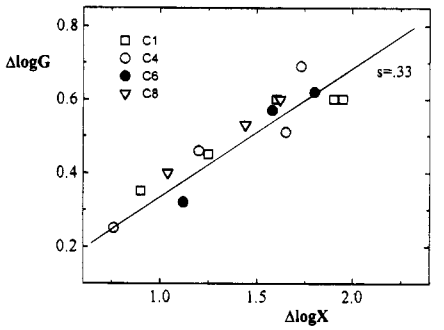

Figure 7. Dependence of the jumpwise change in the modulus, $\Delta \log G$, on the change in the swelling ratio, $\Delta \log X$, at the collapse for gel series C1–C8.

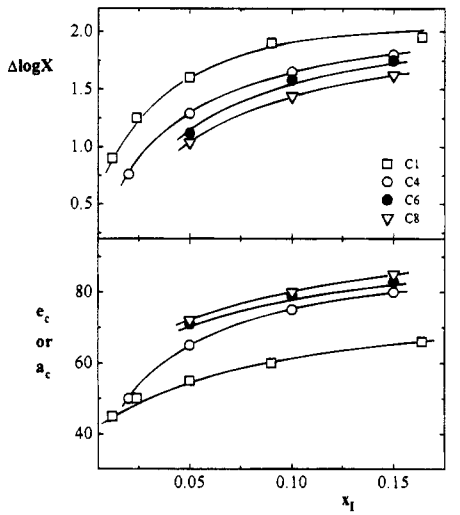

Figure 8. Dependence of the extent of the collapse, $\Delta \log X$, and of the critical ethanol, e_c (series C4, C6, and C8), or acetone, a_c (series C1), concentrations on the molar concentration of **I**, x_I.

Figures 6 and 7 it follows that mechanical behavior is predominantly determined by the degree of swelling of the gel.

The dependence of the extent of the collapse $\Delta \log X$ and of the critical ethanol, e_c, or acetone, a_c, concentrations on the **I** concentration, x_I, can be seen in Figure 8. As expected, $\Delta \log X$ and e_c or a_c values increase with x_I. An increasing length of alkyl decreases $\Delta \log X$ values at constant x_I, while the e_c values in C4, C6, and C8 series slightly increase with n. This means that hydrophobic interactions stabilize the expanded state of the gel and that an enhanced ethanol content in the water–ethanol mixture is needed to bring about the collapse. It may be assumed that e_c increases as a result of preferential sorption of ethanol by hydrophobic regions. It is interesting to note that a_c values of series C1 are considerably lower than e_c values.

Different swelling and mechanical behavior can be seen in Figures 4 and 5 for series C12 and C16. In this case the dependences of $\log X$ and $\log G$ on the ethanol content are continuous for all **I** concentrations x_I. An unexpected slight increase in $\log X$ values (decrease in swelling) with increasing salt concentration is observed for both series at low ethanol concentrations in the mixture. This finding means that the effect of ion on swelling is overcompensated by the effect of hydrophobic interactions from long alkyls.

Wtih exemption of three networks of series C16 with the highest x_I values, the moduli G_1 measured after network formation prior to swelling in water–ethanol

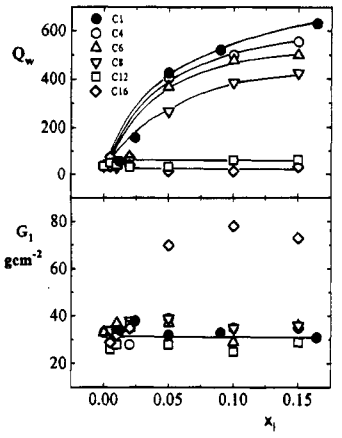

Figure 9. Dependence of the swelling degree in water relative to the dry state, $Q_w = 20/X$, and of the modulus after polymerization, G_1, on the molar concentration of **I**, x_I, for series C1–C16.

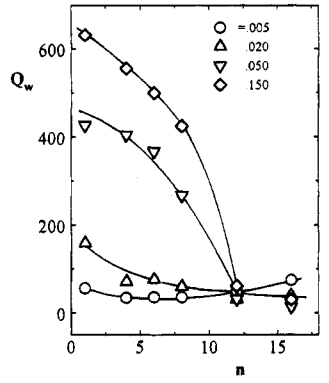

Figure 10. Dependence of the swelling degree in water, Q_w, on the number of alkyl groups in the side chain, n, of **I** for various concentrations x_I.

mixtures are virtually independent of the salt concentrations x_I and of the alkyl length (Figure 9). The concentrations of elastically active chains related to the dry state ν_d are low (Table 1) and indicate a low efficiency of the cross-linking reaction, which is a consequence of large cyclization caused by high dilution. Table 1 shows that the cross-linking efficiency is roughly independent of the alkyl length and **I** concentration. Similar ν_d values ($\nu_d \sim 3.5 \times 10^{-5}$ mol cm^{-3}) were found earlier[3] for various PAAm systems. Due to the distinct amphiphilic character of **I**, $n = 16$, for C16 networks with $x_I \geq 0.05$ the formation of micelles, which can increase the modulus G_1 (or ν_d), is probable. It is interesting to mention that an increase in G_1 has no specific effect on the log G vs log X dependence of C16 networks swollen in water–ethanol mixtures (Figure 6).

As expected for gel series C1, C4, C6, and C8, the swelling degree in water Q_w increases with increasing **I** concentrations x_I (Table 1 and Figure 9). Generally, with increasing length of alkyl at constant x_I, the value of Q_w slightly decreases probably due to the increasing strength of hydrophobic interactions which can be proportional to the number of alkyl groups in salt. On the other hand, for series C12 and C16 the swelling degree Q_w is roughly independent of x_I which means that the polyelectrolyte effect of **I** is compensated by the hydrophobic interactions of the alkyls, which can form micellelike aggregates in the network. The same conclusion can be made from the dependence of Q_w on the number of carbon atoms in the alkyl of **I** shown in Figure 10. As expected, Q_w decreases with n and for $n \geq 12$ Q_w reaches roughly constant minimum values for all x_I, in some cases even lower than Q_w found for an uncharged PAAm network (Table 1).

Comparison between the Theory of Swelling Equilibria of Polyelectrolyte Networks and Experiment. About 20 years ago a modification of the theory of polymer network swelling equilibrium for the polyelectrolyte effect was suggested.[24] In this theory not only the mixing term, P_{os}, given by the mixing of network ions with the solvent in swelling (which is generally used in the literature[1,2]) but also the electrostatic term, P_{elst}, determined by the change of the electrostatic interactions (repulsion) of charges on the chain with swelling were considered in the swelling pressure P. This theory has predicted swelling pressure in the form[3,7,24]

$$P = \mu_1/V_1 = P_m + P_{el} + P_{os} + P_{elst} \qquad (5)$$

where μ_1 is the chemical potential of the solvent, V_1 is the molar volume of the solvent, P_{el} is the elastic term given by a change in the free elastic energy of the chain with swelling and P_m is the mixing term given by the mixing of chain segments with solvent in swelling described by the Flory–Huggins interaction parameter χ. This theory was used for the theoretical description of a collapse phenomenon,[3,7] and it was shown that in the first approximation it describes data obtained poly(acrylamide-*co*-sodium methacrylate) ionic networks.[3,17]

In the theory published earlier[7,24] the individual terms P_i of eq 5 were expressed in molecular parameters characterizing the network structure (concentration of chains ν_d, density of dry polymer ϱ, degree of ionization α, molecular weight of a monomeric unit M_0, molar volume of the water–ethanol mixture V_1, dilution at network formation v^0, dielectric constant ϵ) and in experimental values of the volume fraction of the swollen network $v_2 = 1/Q$. Using eq 5, the dependence of the interaction parameter χ on v_2 was calculated from experimental v_2 values (as the data were obtained for the free swelling $P = 0$ in eq 5) by employing the same procedure described in detail earlier.[3,17]

The use of eq 5 for the PAAm network without **I** (series C4, $x_I = 0$) swollen in pure water ($v_2 = 1/Q_w$; Table 1) led to the expected value of the interaction parameter $\chi = 0.48$. Similarly as before,[3,17] for water-swollen network series C1, C4, C6, and C8 with $x_I > 0$, eq 5 gave high unrealistic values of the χ parameters. Since χ is a measure of the polymer–water interaction when all charges are screened (the effect of charges in eq 5 is considered in P_{os} and P_{elst} contributions), $\chi = 0.48$ may be, in the first approximation, required also for ionic water-swollen networks. This requirement can be met by assuming that the effective degree of ionization α is lower than the **I** concentration x_I, i.e., $\alpha = x_I\phi$, where ϕ is the empirical correlation factor (Table 1). The ϕ values thus calculated lie in the range 0.10–0.35 and are lower than those found for P(AAm/MNa) networks[17] ($\phi = 1$–0.95) and variously aged PAAm networks[22] ($\phi = 0.99$–0.51). [The correction parameter ϕ is related to the activity coefficient of counterions and may involve effects connected with a certain heterogeneity of diluted networks or with other effects not considered in the theory. In the case of variously aged PAAm and P(AAm/MNa) networks the value of $\chi = 0.48$ can be expected because one cannot expect that low content (1–5 mol %), nonionized acrylic or methacrylic acid will affect χ to any marked extent. In the case of measured ionic networks, especially with C8 salt, it is more realistic to assume that χ could increase in uncharged copolymer

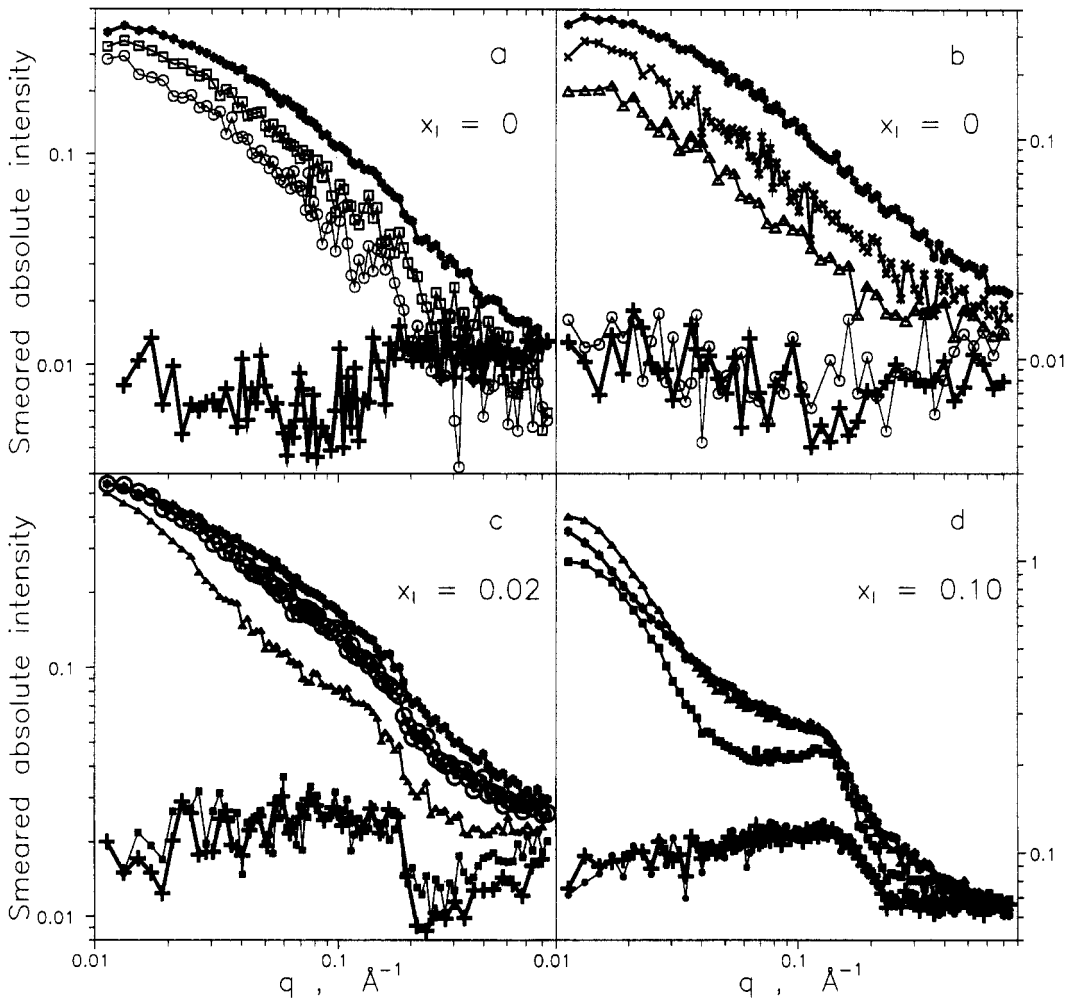

Figure 11. Time-resolved experimental (smeared) SAXS curves taken during network formation in C16 system at indicated values of I concentrations, x_I. Reaction time (s): 100–200 (○), 200–300 (□), 300–400 (△), 400–500 (×), 1400–1600 (●), 1600–2100 (■), 2100–2600 (▲), 2600–3100 (⊙), final state (*) (+, solution without TEMED). (a) Solution flushed with nitrogen for 60 min. (b–d) Regularly prepared solutions.

networks with increasing salt content. On the other hand, no systematic decrease of ϕ with increasing salt content is seen for C1, C4, C6, and C8 salts in Table 1.]

If average values of ϕ are calculated for individual series of networks, then the values ϕ = 0.24, 0.18, 0.15, and 0.12 for series C1, C4, C6, and C8, respectively, are found. Thus increasing the length of alkyl, which decreases the effect of the charge on swelling due to the increasing strength of hydrophobic interactions, lowers the ϕ values. For series C12 and C16 with the longest alkyls eq 5 cannot be successfully applied because, due to the presence of micelles, in many cases the Q_w values of water-swollen ionic networks are lower than the Q_w of an uncharged PAAm network. For network series C12 and C16 where the swelling degree showed a small increase in Q_w with ionization, very low ϕ values are obtained with the exception of two samples with the lowest salt concentration x_I = 0.005 (Table 1). An assumption that concentration x_I = 0.005 is below the critical salt concentration for micelle formation can explain the high degree of swelling of these samples (see SAXS experiments).

Small-Angle X-ray Scattering. Figure 11 shows the SAXS curves recorded during polymerization of three networks of series C16 and x_I = 0, 0.02, and 0.10, respectively. To characterize the course of the polymerization, we plotted also sums of the smeared scattering intensities taken over interval q = 0.02–0.2 Å^{-1} as a function of reaction time (Figure 12).

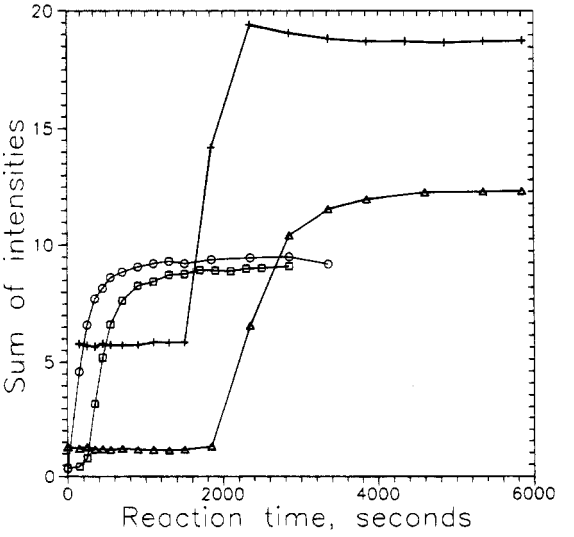

Figure 12. Sum of the SAXS intensities taken over interval m = 0.1–1 cm in dependence on the reaction time for the C16 system. x_I: 0 (○, bubbled with nitrogen), 0 (□), 0.02 (△), 0.10 (+).

Scattering experiments started with solutions containing all the reaction components except TEMED. As expected, the scattering intensities for the solutions with x_I = 0 are very low and do not depend on scattering angle. Higher intensities and a broad maximum are

observed for both samples containing quaternary salt **I**. While the intensity increases with increasing x_I, the shape of the scattering curve is roughly the same for both samples with $x_I > 0$. This behavior indicates that **I** with long alkyl chain forms micelles in the reaction mixture.

Addition of TEMED did not lead to any observable changes in the scattering curves within an initial time period. This period is very short for the sample with $x_I = 0$ bubbled with nitrogen for 60 min (<100 s). It can be seen from Figure 12 that the presence of oxygen lengthens the initial period. The presence of **I** also significantly increases the initial period, and for the samples with **I** (x_I = 0.02 and 0.10) the onset of polymerization is observed after approximately 30 min. The scattering intensities cease to vary with time after about 1.5 h. Therefore, the reaction time used (24 h) is sufficient for full conversion.

Scattering patterns obtained for the samples with $x_I = 0$ (Figure 11a,b) have a form typical of swollen networks after the initial time period. The scattering curves corrected for collimation errors (not shown here) can be approximated by a Lorentzian-type scattering function

$$I(q) = I(0)/(1 + q^2\xi^2) \tag{6}$$

where ξ is the correlation length. At the early stages of polymerization ($t \geq 100$ s for part a and $t \geq 200$ s for part b) we determined $\xi = 60$ Å. With proceeding polymerization the correlation length decreases to its final value $\xi = 35$ Å. This behavior is a consequence of the increase in polymer concentration.

For the sample with higher **I** content ($x_I = 0.10$) scattering curves reveal the existence of micelles both in the polymerization mixture and at the onset of polymerization, and these micelles are clearly preserved also in the gel (Figure 11d). Scattering curves for the sample with $x_I = 0.02$ (Figure 11c) also suggest the existence of micellar structures after polymerization although the micellar contribution is less pronounced due to the large network contribution to scattering intensity. Formation of micelles in the cationic surfactant *N*-alkylpyridinium chloride with alkyl chains $n \geq 12$ was found earlier[25] by SAXS experiments.

The core–shell spherical model is frequently used as the first approximation of micellar structure. In our case, alkyl chains are assumed to form a dense core (radius R_c), while the shell of radius R_s contains polar heads including counterions and water. Assuming, furthermore, uniform distribution of the scattering length density inside both the core and shell and neglecting interparticle interferences, the scattering intensity of such particles can be expressed by the relation (e.g., ref 26)

$$I(q) = I(0)\{yF(qR_c) + (1 - y)[R_s^3F(qR_s) - R_c^3F(qR_c)]/(R_s^3 - R_c^3)\}^2 \tag{7}$$

where

$$F(x) = 3(\sin x - x\cos x)/x^3 \tag{8}$$

$\Delta b = b - \bar{v}\varrho_0$ is the excess scattering amplitude, b and $\bar{v}$ are respectively the scattering amplitude and partial specific volume of the dissolved compound, ϱ_0 is the scattering density of the solvent, $y = \Delta b_c w_c/(\Delta b_c w_c + \Delta b_s w_s)$ is the ratio of the excess scattering amplitude of the core to that of the whole micelle, and w_c and w_s are the weight fractions of the alkyl chain (core) and polar heads, respectively. The extrapolated intensity can be expressed as

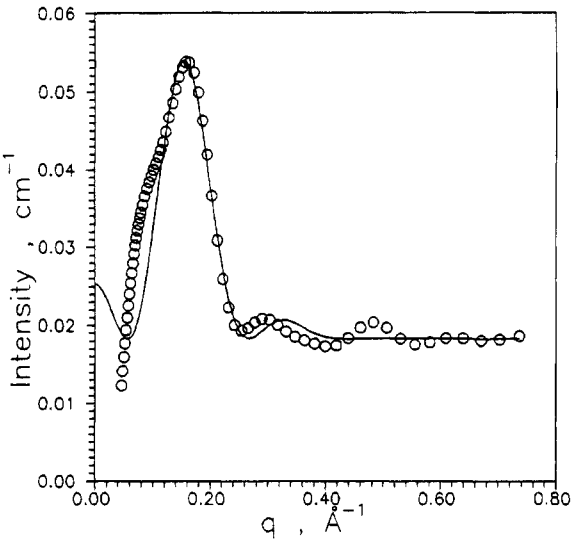

Figure 13. Comparison between the theoretical scattering curve of the core–shell model (solid line) and the experimental desmeared SAXS data (○) of the reaction mixture for the C16 system without TEMED ($x_I = 0.10$). (See text for the values of the micellar structure parameters.)

$$I(0) = (c(\Delta b)^2/N_A)M \tag{9}$$

where c is the particle concentration and N_A is Avogadro's number. The last relation, valid if the interparticle interactions can be neglected, is a basis for the determination of molar mass.

For the system studied we could not determine the micellar mass and size directly because we had not succeeded in obtaining reliable desmeared data in the relevant part of the scattering curve. Glatter's methods for collimation corrections (ITR, ITP) lead to almost identical results for $q > 0.15$ Å^{-1}, but at lower angles the desmeared intensities were strongly dependent on the parameters of the correction process.

The micellar structure parameters could be estimated by fitting eq 7 to the experimental data corrected for collimation errors. Using the partial specific volumes of the quaternary salt, $\bar{v}_{salt} = 0.946$ cm^3/g (ref 27), and of the alkyl chain, $\bar{v}_c = 1.242$ cm^3/g (ref 28), we calculated the excess scattering amplitudes of the core, shell, and whole micelle, respectively (in 10^{10} cm/g): $\Delta b_c = -1.98$, $\Delta b_s = 2.64$, $\Delta b = 0.31$.

The excess amplitude fraction of the core, y, was then estimated to be −3.2. This parameter was kept constant during the fitting process. There are three adjustable parameters related to the micellar structure: $I(0)$, R_c, and R_s. We also adjusted a constant background reflecting the scattering contribution of the acrylamide monomer which was present in the reaction mixture. We used only the desmeared data for $q > 0.15$ Å^{-1}, which are believed not to be affected by uncertainty in collimation corrections and by intermicellar interactions.

The fitting (see Figure 13) resulted in the following values of the parameters: the micelle core radius R_c = 17 Å, the micelle shell radius R_s = 29 Å, the extrapolated intensity $I(0) = 9.0 \times 10^{-3}$ cm^{-1}. Using eq 9, the micelle molar mass of 2.7×10^4 g/mol was estimated. The corresponding aggregation number is 60.

In order to check, to a certain extent at least, the consistency of the above given results, we calculated the radius of the micelle core on the assumption that it contains 60 C16 alkyl chains. Such calculation results in $R_c = 19$ Å, in a reasonable agreement with the value obtained by the scattering curve fitting.

Conclusions

From the swelling, mechanical, and SAXS measurements carried out on the ionic networks of copolymers of acrylamide with quaternary ammonium salts of different alkyl lengths swollen in water–ethanol mixtures, the following conclusions can be made:

(a) Gels from the salts **I** with number of carbon atoms $n = 1-8$ undergo a first-order phase transition; an increase in n stabilizes the expanded state and increases the critical ethanol concentration e_c at which the transition takes place. Increasing the strength of hydrophobic interactions (increasing alkyl length) slightly decreases the degree of swelling in water Q_w and the extent of the collapse $\Delta \log X$ at constant concentration of the salt in gel x_I.

(b) For gels from the salts **I** with $n = 12$ and 16 the swelling degree in water is roughly independent of the concentration of the salt, which means that the polyelectrolyte effect is compensated by hydrophobic interactions of the salts. Scattering curves of gels from **I**, $n = 16$, reveal the existence of micelles for $x_I \geq 0.02$. The micelles contain about 60 molecules. Their structure can be described by the core–shell model with the radii $R_c = 17$ Å and $R_s = 29$ Å.

(c) As the constant amount of cross-linker was used in all networks, the modulus data lie roughly on the same $\log G$ vs $\log X$ dependence regardless of the concentration of the salt **I**. The jump in the modulus at the collapse $\Delta \log G$ adequately correlates with the jump in the swelling ratio $\Delta \log X$ ($\Delta \log G = 0.33\Delta \log X$). This means that mechanical behavior is predominantly determined by the swelling degree for all gels.

Acknowledgment. The financial support of the Grant Agency of the Czech Republic (Grants Nos. 203/93/1057 and 203/95/1318) is gratefully acknowledged.

References and Notes

(1) Shibayama, M.; Tanaka, T. *Adv. Polym. Sci.* **1993**, *109*, 1.
(2) Khokhov, A.; Starodubtsev, S.; Vasilevskaya, V. V. *Adv. Polym. Sci.* **1993**, *109*, 123.
(3) Ilavský, M. *Adv. Polym. Sci.* **1993**, *109*, 173.
(4) Gehrke, S. H. *Adv. Polym. Sci.* **1993**, *110*, 81.
(5) Hirotsu, S. *Adv. Polym. Sci.* **1993**, *110*, 1.
(6) Pleštil, J.; Ostanevich, Yu. M.; Borbely, S.; Stejskal, J.; Ilavský, M. *Polym. Bull.* **1987**, *17*, 465.
(7) Ilavský, M. *Polymer* **1981**, *22*, 1687.
(8) Cussler, E. L.; Wang, K. L.; Burban, J. H. *Adv. Polym. Sci.* **1993**, *110*, 67.
(9) Okano, T. *Adv. Polym. Sci.* **1993**, *110*, 179.
(10) De Rossi, D., Kajiwara, K., Osada, Y., Yamanchi, A., Eds. *Polymer Gels: Fundamentals and Biomedical Applications;* Plenum: New York, 1991.
(11) Suzuki, M.; Hirasa, O. *Adv. Polym. Sci.* **1993**, *110*, 241.
(12) Siegel, R. A. *Adv. Polym. Sci.* **1993**, *109*, 233.
(13) Tanford, C. *The Hydrophobic Effect*; Wiley: New York, 1980.
(14) Ilavský, M.; Hrouz, J.; Havlíček, I. *Polymer* **1985**, *26*, 1514.
(15) Saito, S.; Kanno, M.; Inomata, H. *Adv. Polym. Sci.* **1993**, *109*, 207.
(16) Ilavský, M.; Bouchal, K.; Hrouz, J. *Polym. Bull.* **1990**, *24*, 619.
(17) Ilavský, M. *Macromolecules* **1982**, *15*, 782.
(18) Cheremukhina, G. A.; Chernenko, S. P.; Ivanov, A. B.; Peshekhonov, V. D.; Smykov, L. P.; Zanevsky, Yu. V.; Richter, M.; Traeber, B.; Than Tran Duc *Isotopenpraxis* **1990**, *26*, 547.
(19) Kratky, O.; Pilz, I.; Schmitz, P. J. *J. Colloid Interface Sci.* **1966**, *21*, 24.
(20) Glatter, O.; Gruber, K. *J. Appl. Crystallogr.* **1993**, *26*, 512. Glatter, O. *J. Appl. Crystallogr.* **1977**, *10*, 415.
(21) Dušek, K.; Prins, W. *Adv. Polym. Sci.* **1969**, *6*, 1.
(22) Ilavský, M.; Hrouz, J.; Stejskal, J.; Bouchal, K. *Macromolecules* **1984**, *17*, 2868.
(23) Ilavský, M.; Bouchal, K. In *Biological and Synthetic Polymer Networks;* Kvamer, O., Ed.; Elsevier: New York, 1988; p 435.
(24) Hasa, J.; Ilavský, M.; Dušek, K. *J. Polym. Sci., Polym. Phys. Ed.* **1975**, *13*, 253.
(25) Okuzaki, H.; Osada, Y. *Polym. Gels Networks* **1994**, *2*, 267.
(26) Pleštil, J.; Pospíšil, H.; Ostanevich, Yu. M.; Degovics, G. *J. Appl. Crystallogr.* **1991**, *24*, 659.
(27) Sikora, A. Unpublished results.
(28) Vass, Sz.; Török, T.; Jákli, Gy.; Berecz, E. *J. Phys. Chem.* **1989**, *93*, 6553.

MA9502415